Inorg. Chem. **2004**, *43*, 7061–7067

Electronic Interaction in an Outer-Sphere Mixed-Valence Double Salt: A Polarized Neutron Diffraction Study of $K_3(MnO_4)_2$

Roderick D. Cannon, Upali A. Jayasooriya, and Claire Tilford

School of Chemical Sciences, University of East Anglia, Norwich NR4 7TJ, U.K.

Christopher E. Anson

Institut für Anorganische Chemie II, Universität Karlsruhe, Engesserstrasse Geb. 30.45, D-76128 Karlsruhe, Germany

Frank E. Sowrey*

School of Physical Sciences, University of Kent at Canterbury, Canterbury CT2 7NR, U.K.

David R. Rosseinsky

School of Chemistry, University of Exeter, Stocker Road, Exeter EX4 4QD, U.K.

John A. Stride, Francis Tasset, Eric Ressouche, and Ross P. White

Institut Max Von Laue-Paul Langevin, 6 rue Jules Horowitz, BP 156X, 38042 Grenoble Cedex 9, France

Rafik Ballou

Laboratoire Louis Néel, CNRS, 25 Avenue des Martyrs, BP 156, 38042 Grenoble Cedex 9, France

Received June 11, 2004

The mixed-valence double salt $K_3(MnO_4)_2$ crystallizes in space group $P2_1/m$ with $Z = 2$. The manganese centers Mn1 and Mn2 constitute discrete "permanganate", $[Mn^{VII}O_4]^-$, and "manganate", $[Mn^{VI}O_4]^{2-}$, ions, respectively. There is a spin-ordering transition to an antiferromagnetic state at ca. $T = 5$ K. The spin-density distribution in the paramagnetic phase at $T = 10$ K has been determined by polarized neutron diffraction, confirming that unpaired spin is largely confined to the nominal manganate ion Mn2. Through use of both Fourier refinement and maximum entropy methods, the spin on Mn1 is estimated as $1.75 \pm 1\%$ of one unpaired electron with an upper limit of 2.5%.

Introduction

As part of our ongoing work on electron delocalization and its role in electron transfer reactions, we wished to measure directly the distribution of unpaired electron density in a mixed-valence complex. The technique of polarized neutron diffraction (PND) permits a direct measurement of magnetization density in a crystalline material;[1a] the pioneering application to valence delocalization in a mixed-valence solid was by Day et al. in 1980.[1b] In the absence of orbital angular momentum in the ground state, the magnetization density arises from the unpaired electron ("spin") density. In most transition-metal complexes, orbital angular momentum is largely quenched from the ground state by ligand field effects. We sought a homometallic mixed-valence material

* Author to whom correspondence should be addressed. E-mail: f.e.sowrey@kent.ac.uk. Phone: +44 1227 764000 ext 3776. Fax: +44 1227 827558.

(1) (a) Brown, P. J. *Int. J. Mod. Phys.* **1993**, *137*, 3029. (b) Day, P.; Herren, F.; Ludi, A.; Güdel, H. U.; Hulliger, F.; Givord, D. *Helv. Chim. Acta* **1980**, *63*, 148.

10.1021/ic0492340 CCC: $27.50
Published on Web 10/02/2004

in which the two metal centers have the same coordination spheres, are not linked by bridging ligands, and differ in oxidation state by only one electron. The mixed-valence double salt $K_3[Mn^{VI}O_4][Mn^{VII}O_4]$ **(1)** fulfills all of these criteria; indeed as far as we know it is the only one to do so. It has the additional advantage that the metal centers have configurations d^1 and d^0 so that we are concerned only with the distribution of one electron over the two sites, and the detection of any magnetization on the Mn^{VII} center would be prima facie evidence of delocalization. Formally, it approximates closely to a quasi-symmetrical outer-sphere electron-transfer system, and it provides a solid-state analogue[2−4] of the contact configuration of the electron-transfer reaction between manganate and permanganate ions in solution:[5]

$$MnO_4^- + MnO_4^{2-} \rightleftharpoons MnO_4^{2-} + MnO_4^- \qquad (1)$$

Compound **1** was first prepared in 1860 by Gorgeu[6a] and de Sénarmont,[6b] but it was not studied again until Erenburg et al. reported that the infrared spectrum was consistent with the presence of distinct manganate and permanganate units in the crystal.[7] Powder X-ray diffraction, on this[8a] and analogous Rb and Cs salts,[8b] suggested a rhombohedral space group, apparently isomorphous either with $Ba_3(AsO_4)_2$ ($R3m$) or, more significantly, with $K_3[Cr^{VI}O_4][Mn^{VII}O_4]$ ($R3m$).[9] However, a single-crystal X-ray diffraction study[2] has since shown that the true space group of the present compound is in fact monoclinic, $P2_1/m$. In the asymmetric unit, there are two discrete MnO_4 groups, Mn1 with Mn−O bond lengths similar to those in the structure of $K[Mn^{VII}O_4]$[10a] and Mn2 with Mn−O lengths similar to those in $K_2[Mn^{VI}O_4]$.[10b] They are arranged in pairs with O_3 planes facing each other and with the oxygens in a staggered arrangement to give mixed-valence pseudodimers (Figure 1) that have almost exact D_{3d} symmetry. The dimers, and potassium ions, lie in the crystallographic mirror planes giving exactly coplanar and almost collinear chains −O−Mn−Mn−O−K−K−K−O−Mn−. Between the chains, the dimers are linked by zigzag chains of $[Mn^{VI}O_4]$ units running parallel to the *b* axis. The Mn^{VI}−Mn^{VI} distances within these cross chains are shorter than in K_2MnO_4 (i.e., 4.42 Å). The dimers are also arranged in approximately close-packed layers with their 3-fold axes parallel to each other and perpendicular to the layer. (The symmetry of these layers is exactly 3-fold in the rhombohedral structures.) These layers are stacked in an ABCABC... arrangement, and the K^+ ions in one layer lie very close to

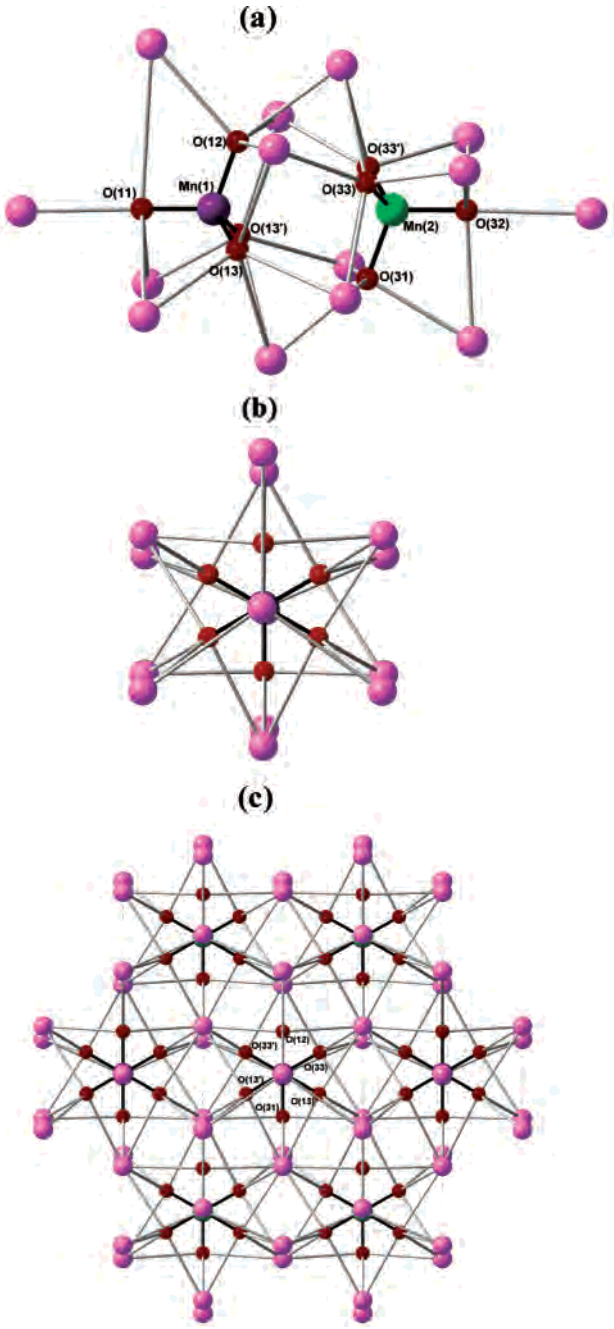

Figure 1. Structure and ionic environment of the {$[MnO_4]\cdots[MnO_4]$} pseudodimer in $K_3[MnO_4]_2$. (a) Viewed along the crystallographic mirror plane, perpendicular to the *b*-axis; (b) viewed along the pseudo-3-fold axis of the dimer.

(2) Hursthouse, M. B.; Quillin, K. C.; Rosseinsky, D. R. *J. Chem. Soc., Faraday Trans.* **1992**, *88*, 3071.
(3) (a) Rosseinsky, D. R.; Stephan, J. A.; Tonge, J. S. *J. Chem. Soc., Faraday Trans.* **1981**, *77*, 1719. (b) Rosseinsky, D. R.; Tonge, J. S. *J. Chem. Soc., Faraday Trans.* **1982**, *78*, 3595.
(4) Cannon, R. D. *Electron Transfer Reactions*; Butterworths: London, 1980. Cannon, R. D. Electron Transfer Reactions, Theory. In *Encyclopaedia of Inorganic Chemistry*; King, R. B., Ed.; John Wiley: New York, 1994; pp 7−9, 10−13, 14−17.
(5) (a) Sheppard, J. C.; Wahl, A. C. *J. Am. Chem. Soc.* **1957**, *79*, 1020. (b) Brit, A. D.; Yen, W. M. *J. Am. Chem. Soc.* **1961**, *83*, 14516. (c) Myers, O. E.; Sheppard, J. C. *J. Am. Chem. Soc.* **1961**, *83*, 4739. (d) Sham, T. K.; Brunschwig, B. S. *J. Am. Chem. Soc.* **1981**, *103*, 1590. (e) Spiccia, L.; Swaddle, T. W. *Inorg. Chem.* **1987**, *26*, 2265. (f) Spiccia, L.; Swaddle, T. W. *J. Chem. Soc., Chem. Commun.* **1985**, 67.
(6) (a) Gorgeu, A. *Compt. Rend.* **1860**, *50*, 610. (b) de Sénarmont, H. *Ann. Chim. Phys.* **1860**, *61*, 357. See also other references cited in Mellor, J. W. *A Comprehensive Treatise on Inorganic and Theoretical Chemistry*; Longmans, Green & Co.: London, 1932; Vol. 12, pp 331, 341.
(7) Erenburg, B. G.; Boldyrev, V. V.; Anikina, L. D.; Mikhailov, Yu. I. *Zh. Strukt. Khim.* **1968**, *9*, 536.
(8) (a) Boldyrev, V. V.; Vinokurova, Z. G.; Senchenko, L. N.; Shchetinina, G. P.; Erenburg, B. G. *Russ. J. Inorg. Chem.* **1970**, *15*, 1341. (b) Erenburg, B. G.; Senchenko, Boldyrev, V. V.; Malysh, A. V. *Russ. J. Inorg. Chem.* **1972**, *17*, 1121.
(9) (a) Stanley, E. *Research* (London), **1952**, *5*, 589−590. Stanley, E. *Chem. Abstr.* **1954**, *48*, 5591f. (b) Stanley, E. *Z. Krystallogr.* **1968**, *127*, 450.
(10) (a) Palenik, G. *Inorg. Chem.* **1967**, *6*, 503. (b) Palenik, G. *Inorg. Chem.* **1967**, *6*, 507.

the extension of the 3-fold axis of a pseudodimer in another layer. It is likely that the twinning that was found to be quite common in crystals of this material ("type B" crystals[2]) results from an "incorrect" stacking of the layers (e.g., ABCABABC...). In summary, the structure of $K_3(MnO_4)_2$ is extremely similar to that of $K_3[CrO_4][MnO_4]$, the difference being that in the present compound deviations from 3-fold symmetry can be discerned.[11]

In a preliminary account of this work,[12] it was concluded that the unpaired electron density is predominantly concentrated on half of the manganese centers, but this did not exclude small densities in the vicinity of the others and the limitations of the method of data analysis did not allow upper limits to be set. The data have now been reanalyzed using both maximum entropy[13,14] and form-factor refinement methods, and we now propose an upper limit of 2.0% delocalization of the unpaired electron from Mn2 to Mn1.

Experimental Section

$K_3(MnO_4)_2$. The solids $KMnO_4$ and K_2MnO_4[10b,15] were added in alternate small portions to warm aqueous 4 M KOH until the mixture was equimolar in the two materials and just below saturation for $KMnO_4$, the less soluble of the two components. With practice, it was possible to judge the equivalence ratio by eye, the "crucial violet" shade[2] being quite distinct from the purple and green of the components though there is no evidence of any chemical interaction. Solutions of ca. 100 mL volume were allowed to evaporate in desiccators at reduced pressure over P_2O_5 at 35 °C for several days. This procedure gave thin plates of approximately hexagonal shape (generally at the surface of the solution) and more equidimensional blocks up to 3 mm long at the bottom of the evaporating dish. Infrared spectra were recorded on a Mattson FT-IR spectrometer using KBr disks at liquid nitrogen temperature under dry nitrogen to avoid contamination with CO_2. Typical well-formed crystals were selected for the IR measurements, and the spectra were compared with those of freshly crystallized $KMnO_4$ and K_2MnO_4, as noted below. Because previous work[2] had indicated that crystals of the mixed-valence compound are frequently twinned, a number of crystals were examined using a Weissenberg camera. The crystal selected, of approximate dimensions $3.0 \times 2.5 \times 1.8$ mm^3, gave a Weissenberg pattern that could be indexed in terms of the unit cell of the untwinned structure.

(11) The rhombohedral cell can be transformed into the monoclinic by the matrix

$$\begin{matrix} 1 & 0 & 0 \\ 0 & -1 & 1 \\ 1 & -1 & -1 \end{matrix}$$

This transformation involves the loss of two of the three mirror planes (and thus the 3-fold symmetry) to give a *C*-monoclinic cell (*C*2/*m*). Further loss of the 2-fold axes (and with them the lattice centering) gives the observed $P2_1/m$ unit cell.

(12) Cannon, R. D.; Jayasooriya, U. A.; Anson, C. E.; White, R. P.; Tasset, F.; Ballou, R.; Rosseinsky, D. R. *J. Chem. Soc., Chem. Commun.* **1992**, 1445.

(13) (a) Papoular, R. J.; Gillon, B. In *Neutron Scattering Data Analysis 1990*. Int. Phys. Conf. Ser. No 107; Johnson, M. W., Ed.; Chapter 2, p 101. (b) Papoular, R. J.; Gillon, B. *Europhys. Lett.* **1990**, *13*, 429. (c) Papoular, R. J.; Zheloudev, A.; Ressouche, E.; Schweizer, J. *Acta Crystallogr.* **1995**, *A51*, 295. (d) Zheludov, A.; Papoular, R. J.; Ressouche, E.; Schweizer, J. *Acta Crystallogr.* **1995**, *A51*, 450.

(14) (a) Ressouche, E.; Schweizer, J. *J. Neutron Res.* **1996**, *4*, 15. (b) Ressouche, E. *Physica B* **1999**, *267*−*268*, 27. (c) Ressouche, E. *J. Phys. Chem. Solids* **2001**, *62*, 2161.

(15) Scholder, R.; Waterstradt, H. *Z. Anorg. Allg. Chem.* **1954**, *277*, 172.

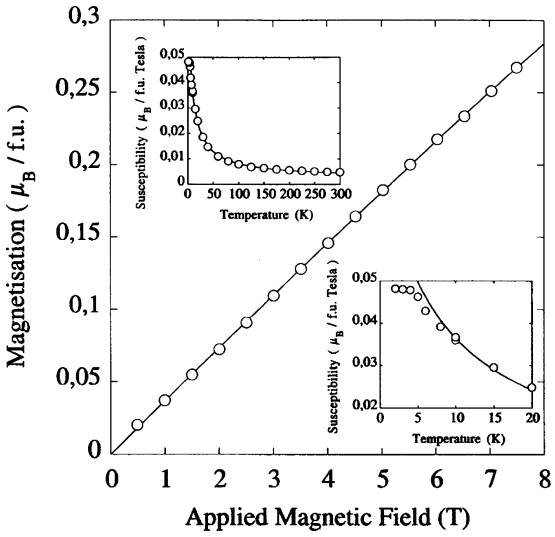

Figure 2. Magnetization isotherm for $K_3[MnO_4]_2$, $T = 10$ K. Insets: Temperature dependence of magnetic susceptibility, χ_1, as defined in the text.

Measurements. Magnetic Susceptibility. Bulk magnetization was measured at the Laboratoire Louis Néel, CNRS, Grenoble, on a purpose-built magnetometer using the anti-Helmholz two-coil extraction method. The applied magnetic field *B*, supplied by a superconducting magnet, was varied up to 8 T. The temperature at the sample was varied, using a helium flow cryostat, over a range 2 to 300 K. Figure 2 shows the magnetization isotherm for 10 K. The experimental data gave an excellent fit to the empirical polynomial expression $M = \chi_1 B + \chi_3 B^3$, with the initial susceptibility $\chi_1 = 0.03666\mu_B$ T^{-1} per formula unit, and a negligible third-order susceptibility (ca. $\chi_3 = -2 \times 10^{-5}\mu_B$ T^{-3} per formula unit where μ_B = Bohr magneton $= eh/2m_e = 9.274 \times 10^{-24}$ J T^{-1} and where e and m_e are the charge and rest mass of the electron).

Also shown in Figure 2 (insets) is the thermal variation of the initial magnetic susceptibility χ_1 as deduced from the isotherms measured at different temperatures. From ca. $T = 8$ K upward, it follows the modified Curie−Weiss law

$$\chi = \chi_0 + \frac{C}{T - \theta} \qquad (2)$$

with $\chi_0 = 0.0018(2)\mu_B$T^{-1}per formula unit. The Curie constant is $C = 0.66(2)\mu_B$ K T^{-1} per formula unit, which leads to an effective moment $\mu_{eff} = 1.73(2)\mu_B$, as compared with the spin-only value $g[s(s+1)]^{1/2} = \sqrt{3} = 1.732\mu_B$. The negative θ value of −9.5(7) K implies that there should be antiferromagnetic correlations in the sample at low temperatures, and this is confirmed by the anomalies in the thermal variation of χ_1 at temperatures below 8 K. The data plotted in Figure 2 (inset) indicate a Néel temperature of ca. 5 K, in agreement with other experiments referred to below.

Nuclear Structure. The nuclear structure was refined at $T = 10$ K by neutron diffraction, using the instrument D15 at the ILL, Grenoble. Reflections were measured with $h = -9$ to 0, $k = -2$ to 0, and $l = 0$ to 12, giving a total of 477 unique, accepted reflections. Extinction parameters were refined from the D15 experimental data, and the data were corrected for extinction. The data were corrected for absorption using analytical methods. Taking the room temperature structure as an initial set of parameters, all atoms were refined anisotropically to weighted values $R = 0.019$, $R_w = 0.008$ (where $R = \{\sum||F_o| - |F_c||\}/\{\sum|F_o|\}$ and $R_w = \{\sum w^{1/2}||F_o| - |F_c||\}/\{\sum w^{1/2}|F_o|\}$, $w^{-1} = \{s^2(F_o) + g\{F_o\}^2\}$). Cell parameters were obtained as $a = 7.809(14)$, $b = 5.742(6)$, and $c =$

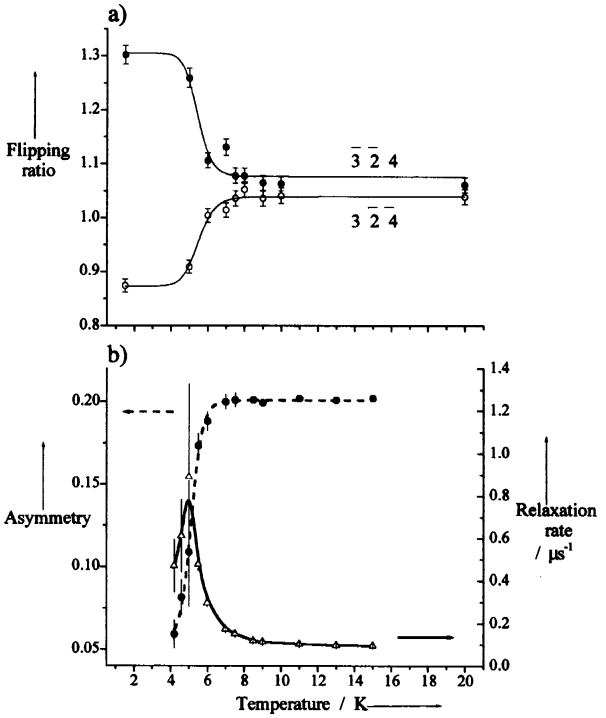

Figure 3. Evidence of the magnetic phase transition in $K_3[MnO_4]_2$: (a) neutron flipping ratios for 3−2−4 and 3−2−4 reflections, measured on D3b at ILL with an applied field of 4.6 T; (b) muon spin relaxation times, measured on the instrument EMU at the Rutherford Appleton Laboratory, Chilton, Didcot, UK. (See ref 15.)

9.721(13) Å, and $\beta = 112.14(4)$ deg. The corresponding parameters found by X-ray diffraction at room temperature were $a = 7.868(1)$, $b = 5.783(1)$, and $c = 9.7897(1)$ Å, and $\beta = 112.00(1)°$. A similar set of data was collected at 1.5 K. Thus, there is no change in the symmetry of the nuclear structure over the three temperatures measured and no significant change in cell parameters between 10 and 1.5 K.

Polarized Neutron Diffraction. The experiment was carried out on the instrument D3b at the ILL. The chosen crystal was mounted on a goniometer and coated with silicone grease to inhibit reaction with oxygen and more especially with water vapor. After optical alignment, it was transferred directly to an aluminum pin, and the alignment was checked using a Laue camera. The mounted crystal was transferred to the cryostat of D3b with the *b* axis vertical and perpendicular to the neutron beam. It was centered using 15 reflections that were initially located from the room-temperature X-ray data. Flipping ratios $R(hkl)$ were measured with an applied field of 4.6 T. The ratios $R(3, -2, -4)$ and $R(-3, -2, 4)$ were calculated to be the most sensitive to temperature and were measured at different temperatures over the range 1.5 to 40 K. The results of this scan are shown in Figure 3. It was immediately clear that at low temperature the ratios were not equivalent for (h, k, l) and $(-h, k, -l)$ outside the $k = 0$ layer. For example, at $T = 1.5$ K the ratios $R(3, -2, -4)$ and $R(-3, -2, 4)$ were 0.88(1) and 1.32(2), respectively. As the temperature was raised, the two ratios converged at ca. 10 K. This indicated a phase transition at ca. 5−6 K, the lower-temperature phase being of lower symmetry than $P2_1/m$ (by loss of the 2_1 axis and probably also the mirror plane to give triclinic $P\bar{1}$) and thus necessarily antiferromagnetic. This is consistent with the MuSR experiments referred to below, which also indicated low-temperature antiferromagnetism and a Néel point of 5.1 K. Further values of $R(hkl)$ were then measured for reflections with $h = -9$ to 0, $k = -2$ to 0, and $l = 0$ to 12 at $T = 10$ K all with $H = 4.6$ T. The ratio $\gamma(hkl) = M(hkl)/N(hkl)$ between the magnetic and nuclear structure factors was calculated for each (hkl) reflection. Fourier components $M(hkl)$ of the magnetization distribution were finally deduced by setting the $N(hkl)$ to the values refined from the D15 experiment. $M(000) = 0.1666(2)\mu_B$ was provided by the bulk magnetization measurements.

Table 1. Mn−O Bond Distances (Å) and Mn−O−Mn Angles (deg) in MnO_4 Ions in $K_3(MnO_4)_2$ at $T = 10$K

	permanganate		
Mn(1)−O(11)	1.612	O(11)−Mn(1)−O(12)	109.2
Mn(1)−O(12)	1.622	O(11)−Mn(1)−O(13)	109.5[a]
Mn(1)−O(13)	1.629[a]	O(12)−Mn(1)−O(13)	109.2[a]
		O(13)−Mn(1)−O(13′)	110.1
mean	1.623		109.45
sd[b]	0.007		0.3
	manganate		
Mn(2)−O(21)	1.661	O(21)−Mn(2)−O(22)	109.9
Mn(2)−O(22)	1.649	O(21)−Mn(2)−O(23)	109.1[a]
Mn(2)−O(23)	1.664[a]	O(22)−Mn(2)−O(23)	110.0[a]
		O(23)−Mn(2)−O(23′)	108.7
mean	1.660		109.5
sd[b]	0.006		0.5

[a] ×2. [b] sd = standard deviation of the four or six parameters; individual esd's are not taken into account.

Results

The structural data are of interest because they provide a direct comparison of the geometries of the two MnO_4 anions in similar crystallographic environments at low temperature. The respective Mn−O distances and O−Mn−O bond angles are compared in Table 1. The mean Mn−O distance is less in the manganate(VII), permanganate, than in the manganate(VI), as expected, and is less by a similar amount as was found in the room-temperature X−ray study of the present compound (mean distances 1.611 and 1.655 Å)[2] and in the separate materials $KMnO_4$ and K_2MnO_4 (1.607 and 1.646 Å, respectively).[10] Although both ions are on C_s sites, so they each have two equivalent atoms, they are both very close to 3-fold symmetry, and the main structural distortion is that in each ion the Mn−O bond along the pseudo-3-fold axis is slightly shorter than the other three. Surprisingly perhaps, the spread of Mn−O distances is less in the manganate(VI) than in the manganate(VII). This confirms what was found at room-temperature but contrasts with $KMnO_4$ and K_2MnO_4, but the spread of bond angles is somewhat greater in the manganate(VI) ion. Calculations of the Jahn−Teller effect due to the unpaired e_g electron in the tetrahedral environment imply that angular distortion is more important than bond length differences,[16] and Brunold and Güdel observed the importance of bending modes in the fine structure of the luminescence spectrum at 15 K.[17] The IR absorption spectrum of $K_3(MnO_4)_2$ shows the mode ν_3 of MnO_4 (ν_d Mn−O) for both ions, both split into three components by the low site symmetry. For manganate(VII), they are sharp at 901, 914, and 927 cm^{-1}; for manganate(VI), they are relatively broad at 811, ca. 820, and 831 cm^{-1}. These features

(16) Atanasov, M. Z. *Z. Phys. Chem.* **1997**, *200*, 57.
(17) Brunold, T. C.; Güdel, H. U., Riley, M. J. *J. Chem. Phys.* **1996**, *105*, 9931. Brunold, T. C.; Hazenkamp, M. F.; Güdel, H. U. *J. Am. Chem. Soc.* **1995**, *117*, 5598. Brunold, T. C.; Hazenkamp, M. F.; Güdel, H. U. *J. Lumin.* **1997**, *72−74*, 164.

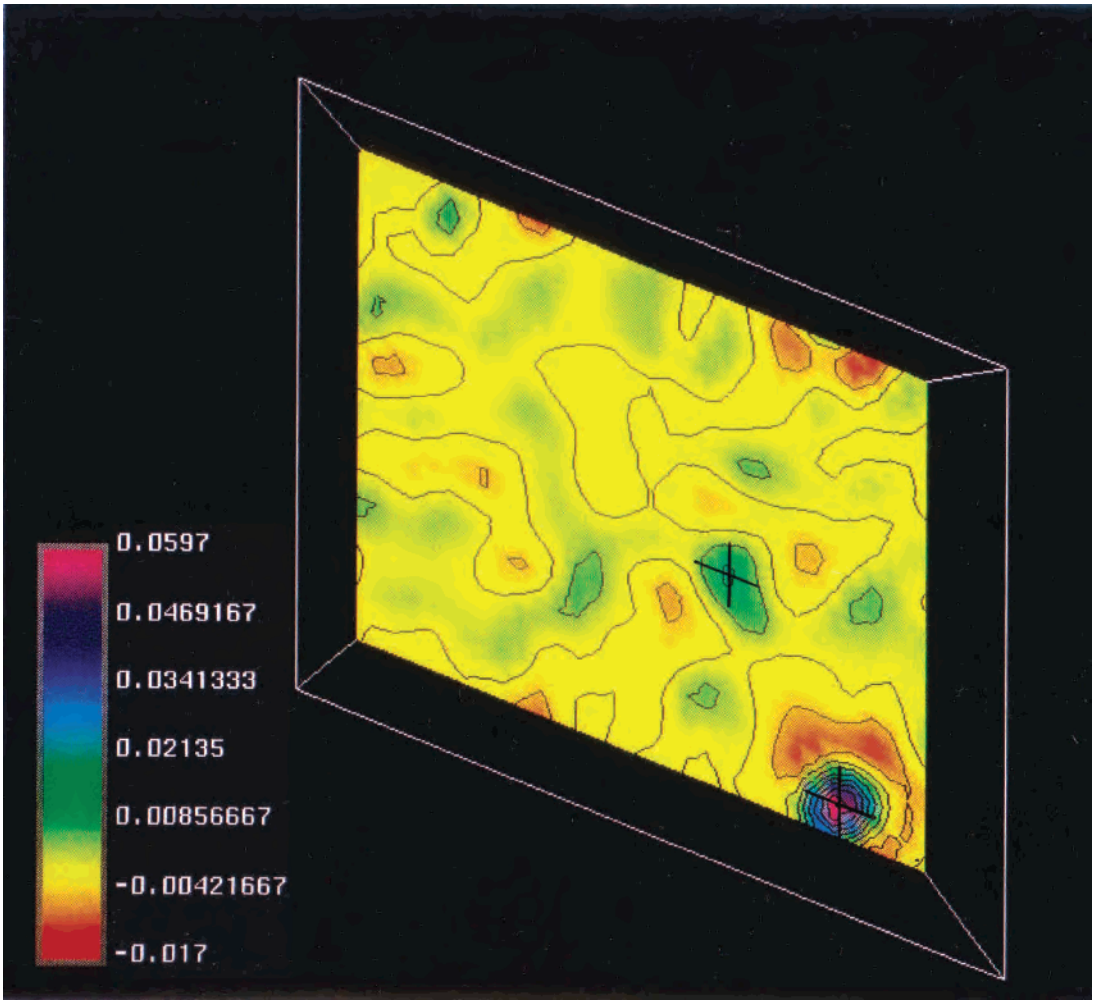

Figure 4. Magnetization density map of $K_3(MnO_4)_2$, calculated by Fourier refinement from polarized neutron diffraction data obtained on D3b at ILL; $T = 10$ K. Cross section in the xz plane at $y = 0.75$. The crosses show positions of atoms Mn1 and Mn2 calculated from unpolarized neutron diffraction data obtained on D15 at ILL; $T = 10$ K.

are identical to those observed in spectra of $KMnO_4$ and K_2MnO_4 measured on the same instrument at the same temperature.

All polarized neutron experiments of the kind reported here yield magnetic structure factors, which are the Fourier components of the magnetization distribution, and the general problem of retrieving the distribution in real space is a Fourier inversion.[13d] The available methods are broadly of two kinds, "direct" methods that involve no a priori model and refinement methods using a model based on existing information. Direct methods based on Fourier inversion have certain well-known drawbacks. They take no account of uncertainties in the experimental data, and they involve setting all unmeasured coefficients (i.e., reflections too weak to be observed) to zero. This can lead to artifacts in the reconstructed map. Methods based on the maximum entropy criterion avoid these problems. However, when the aim is to establish limiting values for densities that are not actually detected, the model refinement methods do have the apparent advantage of yielding standard errors of estimate in the conventional statistical sense. In this work, both approaches have been used.

"Classical" Fourier Inversion. Preliminary reconstruction of the magnetization distribution had already indicated strong localization at the nominal manganese(VI) centers.[12] The data left open the possibility of a small net magnetization at Mn1, but the low-density contours were rather irregular and not well-related to positions of atoms. It was suspected that they were dominated by artifacts due to truncation errors. Refinement using the nuclear structure factors from the low-temperature neutron diffraction experiment on D15 has, however, given a more intuitively satisfying result. Figure 4 shows a cross section of the magnetization map in the plane $y = 0.75$. The calculated positions on Mn1 and Mn2 in this plane are shown, and it is now clear that whereas the bulk of magnetization density resides on Mn2 there is a significant and well-localized "pool" of density coinciding with the position of Mn1.

In a first attempt to provide numerical estimates of magnetization at the Mn1 site, further refinements were made using a range of estimated magnetic form factors for manganese(VI). The first three estimates used the published free-ion calculations[18] for Mn^{2+}, Mn^{3+}, and Mn^{4+}. Agreement between calculated and observed magnetic structure factors

improved slightly along this series with $R = 15.1$, 13.8, 13.0%. Two more calculations were made, with form factors expressed as $\langle j_0 \rangle = \exp(-As^2)$, in the notation of P. J. Brown.[18] The first estimate used $A = 6.19$ Å^2, based on a manual extrapolation from published values in the sequence Mn^+, Mn^{2+}, Mn^{3+}, Mn^{4+}. The second used the value $A = 7.25$ Å^2, which was found to give the closest agreement ($R = 13.6$, 12.8% respectively). The five estimates of magnetization at Mn1 did not vary greatly, the ratio Mn1/Mn2 being 1.7 ± 1.1, 1.8 ± 1.0, 1.75 ± 0.9, 1.6 ± 1.0, and 1.8 ± 0.9%.

MaxEnt Reconstruction. Figure 5 shows projections of magnetization density on the (100), (010), and (001) planes deduced by the three-dimensional (3D) maximum entropy method.[13,14] It should be noted that in the PNS experiment the range of detector angles is limited in the vertical direction, which is the *b* axis of the crystal in the present experiment. This limits the spatial resolution in that direction. However as demonstrated elsewhere,[13c] the limitation is largely overcome in a MaxEnt calculation that uses the whole of the 3D data set to produce each 2D projection.

The lowest-density contour is set at $0.005\mu_B$ Å^{-2}, and the small areas of magnetization other than that surrounding Mn1 are considered to be insignificant because they do not coincide with any atomic positions. The reconstruction places no magnetization density in the vicinity of Mn1. It does not lead to a finite estimate with "error bars" in the conventional sense, but it does suggest an upper limit in one obvious way. The highest magnetization contour is $0.195\mu_B$ Å^{-2}, and if we assume that the spatial extension of magnetisation would be the same for an electron residing on Mn1 as on Mn2, then the upper limit is simply 0.005/0.195 (i.e., about 2.5%).

Further insight can be obtained by building the reconstruction from a nonuniform prior distribution.[13d] The density maps in Figure 5 were constructed from a starting hypothesis of equal probability of magnetization in each volume element of real space (the "flat prior" distribution). For the nonuniform prior, or default, model we started with 98% of the magnetization localized around Mn2, in a spherical distribution, and the remainder around Mn1. Figure 6a shows the MaxEnt reconstruction obtained in this way, Figure 6b shows the default model, and Figure 6c is the difference between the reconstruction and the model. This difference map shows only features in the region of Mn2. By comparison to the spherical distribution used in the model, a small anisotropy is present in the reconstruction, as expected for one electron in a 3d orbital. No differences are visible around Mn1, and this is an additional confirmation of the 2% upper limit of delocalization from Mn2 to Mn1.

Discussion

The magnetic phase transition evident from the present measurements has been observed independently by another method.[19] Rates of muon spin relaxation (MuSR) pass through a discontinuity at $T = 5.1$ K, as shown in Figure 3.

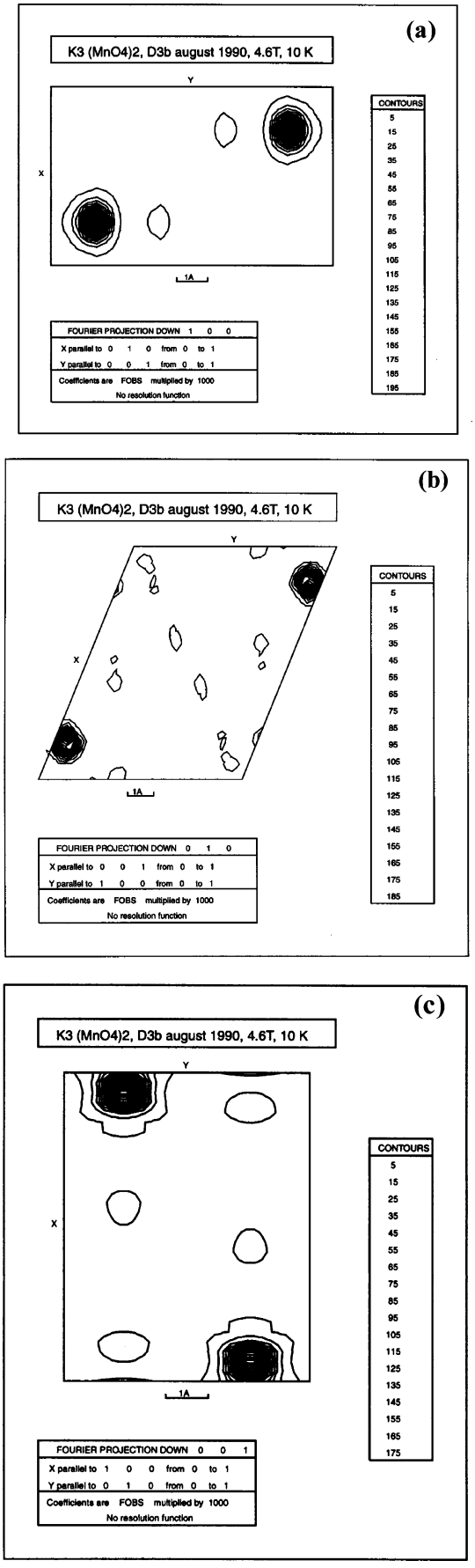

Figure 5. Magnitization density maps of $K_3[MnO_4]_2$, projected on planes (100), (010), and (001). The density was calculated starting from a prior distribution of magnetization, uniform throughout the unit cell.

(18) Brown, P. J. Magnetic Form Factors. In *International Tables for Crystallography*; Wilson, A. J. C., Ed.; Kluwer: Boston, 1992; Vol. C, 391.

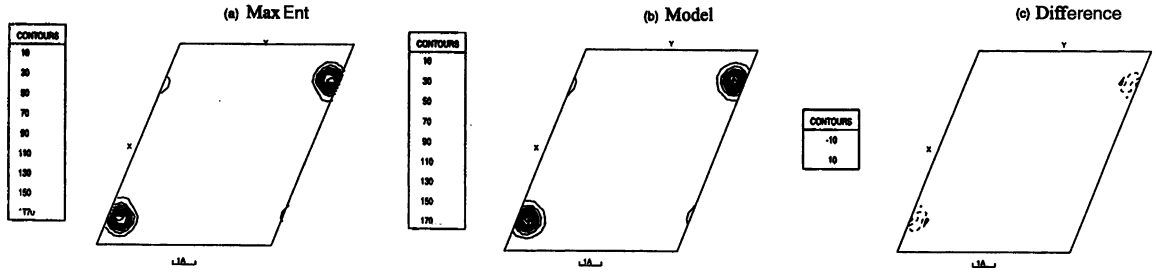

Figure 6. Magnetization density map of $K_3[MnO_4]_2$, projected on the plane (010). (b) Starting model with 98% of the spin concentrated at the Mn2 sites (the contours do not show the 2% that is at the Mn1 sites); (a) model reconstructed by MaxEnt, starting from b; (c) the difference between a and b.

The relaxation rate is sharply sensitive to heterogeneous local magnetic fields. The site of the muon when it localizes in the crystal is not directly determined, but Stride et al.[19] argue that a position in the six-oxygen hole between the two MnO_4 groups is most likely. By calculation of field gradients for several model spin arrangements (all spins being located on Mn1), they ruled out a ferromagnetic structure and favored one of three possible noncanted antiferromagnetic structures. The present results also rule out ferro- (and ferri-) magnetism but do not distinguish between different permutations of upward and downward spins, apart from the requirement of a lower symmetry. We plan to return to this question using neutron diffraction in the low-temperature phase.

With regard to the chemical configuration, there is no doubt that the formula $K_3[Mn^{VII}O_4][Mn^{VI}O_4]$ is an excellent approximation, but there is detectable spin at the location of atom Mn1, confirmed by three independent methods of assessment. These are the close coincidence of the lower maximum in the magnetization density contours to the position of Mn1 in the $y = 0.75$ plane, the concurrence of estimates from Fourier refinement giving a local total equivalent to (1.75 ± 1)% of one electron spin, and the MaxEnt reconstruction placing an upper limit of 2 to 2.5% of one electron, assuming the absence of any contribution from orbital angular momentum.

One contributor to this effect that must not be overlooked is simple disorder in a crystallographic sense, some of the Mn atoms at site 1 being true manganese(VI) with oxygen atoms coordinated at long distance and some of those at site 2 being true manganese(VII) with oxygen atoms coordinated at short distance. We can hardly envisage this happening on a local, microscopic scale (e.g., one pseudodimer being the "wrong way round" relative to its neighbors), but the possibility of the dimers in a small region being misoriented, in what would amount to localized twinning, is physically more reasonable.

In a semiclassical model of electron transfer, delocalization of unpaired electrons is related to interaction between the occupied orbitals of manganese(VI) and the unoccupied orbitals of manganese(VII). With such interaction, the oxidation states would be described as $[Mn^{(6+x)+}\cdots Mn^{(7-x)+}]$ with $x > 0$. Following Mayoh and Day,[20] we may write the wave functions of the transferable electron as

$$\Psi_+ = (1 + \alpha^2)^{-1/2}[\,\alpha\Psi_1 + \Psi_2\,] \qquad (3a)$$

$$\Psi_- = (1 + \alpha^2)^{-1/2}[-\Psi_1 + \alpha\Psi_2] \qquad (3b)$$

where Ψ_1 and Ψ_2 are zeroth-order wave functions for the electron localized on Mn1 and Mn2, respectively, and Ψ_+ and Ψ_- are wave functions for the ground and excited states of the mixed-valence dimer. The electron densities at the two atoms in the ground state are then $(1 - \alpha^2)$ and α^2, respectively, and our results give $\alpha^2 \approx 0.02$. If more cautiously we take the upper limit, then we have $0 < \alpha^2 < 0.025$. There is still scope for a range of physical descriptions within the Robin−Day mixed-valence classes I and II[21] for minimal to zero delocalization or moderate delocalization, respectively. It is at least intriguing to note that the face-to-face arrangement of tetrahedra in the pseudodimer (Figure 1) is ideal for orbital overlap and to note that the Mn1−Mn2 distance of 3.978 Å is considerably shorter than the shortest Mn−Mn distances in $KMnO_4$ or K_2MnO_4, 4.254 and 4.875 Å, respectively.[10a,b] It is also relevant that conductivity and dielectric relaxation measurements on crystal samples of the present compound,[2] and on mixtures of manganates and permanganates,[3,22] albeit at higher temperatures, have demonstrated semiconduction activation energies similar to that of the self-exchange reaction (eq 1) in solution[5e] (48 ± 3 and 46 ± 4 kJ mol^{-1}, respectively). At room temperature and above, the electron-transfer process is apparently adiabatic; whether it remains so down to the low temperatures of this work remains to be determined.

Acknowledgment. This work was presented at the Symposium on Structure and Properties of Novel Compounds on the occasion of the 65th birthday of Professor Peter Day, The Royal Institution, London, September 1−2, 2003. Discussions with Dr. P. J. Brown, Professor G. D. Kearley, and Dr. A. S. Wills are gratefully acknowledged. We thank the ILL and RAL for beam time and the EPSRC for financial support. R.D.C. held a Leverhulme Emeritus Research Fellowship.

Supporting Information Available: Magnetic structure factors, selected atomic coordinates, IR spectra, and output from the polarized neutron diffraction experiments. This material is available free of charge via the Internet at http://pubs.acs.org

IC0492340

(19) Stride, J. A.; Jayasooriya, U. A.; Cannon, R. D.; Bourke, J. P.; Rosseinsky, D. R.; Ballou, R.; Cottrell, S. P. *ChemPhysChem* **2001**, *2*, 683.
(20) Mayoh, B.; Day, P. *J. Am. Chem. Soc.* **1972**, *94*, 2885.
(21) Robin, M. B.; Day. P. *Adv. Inorg. Chem. Radiochem.* **1967**, *10*, 247.
(22) Rosseinsky, D. R.; Muthakia, G. K. *J. Chem. Res.* **2000**, *3*, 116.